Article

Journal of the Brazilian Chemical Society

https://dx.doi.org/10.21577/0103-5053.20250001

J. Braz. Chem. Soc. **2025**, *36*, 5, e-20250001, 1-10

Chitosan Pretreatment: Evidence of Enhanced Mechanical Stability and Adsorption Capacity to Produce a Hybrid Material

Suesslley G. G. Rodrigues,[a] Gisele S. Lopes,[b] Elisane Longhinotti[b,c] and Izaura C. N. Diógenes[*,a]*

[a]*Departamento de Química Orgânica e Inorgânica, Universidade Federal do Ceará, 60455-970 Fortaleza-CE, Brazil*

[b]*Departamento de Química Analítica e Físico-Química, Universidade Federal do Ceará, 60455-970 Fortaleza-CE, Brazil*

[c]*Departamento Acadêmico de Química e Biologia, Universidade Federal Tecnológica do Paraná, 80230-901 Curitiba-PR, Brazil*

Securing a food supply is a global issue that must be integrated into a sustainable framework to mitigate the effects of climate change. This study focuses on the synthesis of a hybrid material for detecting heterocyclic aromatic amines (HAAs), which are potential mutagenic and carcinogenic compounds generated during the heat processing of food. A novel approach was applied to produce films based on chitosan biopolymer incorporated with $[Fe(CN)_5(OH_2)]^{3-}$, CS-Fe, which functions as the active moiety for the detection of quinoxaline (IQx), a molecule similar to HAAs. The pretreatment of the chitosan (CS) films significantly improved mechanical stability and more than doubled the adsorption capacity for $[Fe(CN)_5(OH_2)]^{3-}$. The measurements from real samples indicated that the CS-Fe film can selectively detect IQx, even amidst common interfering amino acids like methionine, tryptophan, and histidine. In summary, the CS-Fe film may be regarded as an eco-friendly and cost-effective material suitable for food safety applications.

Keywords: chitosan, iron complex, hybrid material, quinoxaline, heterocyclic aromatic amines

Introduction

Several sources[1-4] have been warning about the risk of cancer development and mortality in consequence of the consumption of ultra-processed foods (UPF). Among the human carcinogen substances very likely present in UPF, there are heterocyclic aromatic amines (HAAs) which are a large group of over thirty substances. Most HAAs exhibit mutagenic and carcinogenic effects on mammalian cells.[5-7] The International Agency for Research on Cancer (IARC)[8] estimates that daily consumption of 50 g of processed meat may increase the incidence of pancreatic, colon, breast, and prostate cancers by 19, 18, 9, and 4%, respectively. The HAAs compounds are produced during high-temperature cooking of foods rich in protein and creatine, such as meat and fish.[5,9-11] Heat processing of food, while improving desirable aromas, colors, and flavors, also produces potentially mutagenic and carcinogenic compounds, notably the undesirable heterocyclic amines (HAAs).[12] Heat treatment enhances oxidative processes in lipids and proteins by increasing free radical production and reducing the antioxidant protection capacity of food.[13] The toxic substances generated during the heat treatment may interact with deoxyribonucleic acid (DNA), leading to mutations and, consequently, cancer. According to the cooking temperature, HAAs are classified[7,9,11] into two main types: thermal HAAs or IQ (quinoline) type (from 100 to 300 °C) and pyrolytic HAAs or non-IQ type (> 300 °C).

Current methods for detecting HAA are based on chromatographic techniques that can be costly and require the use of organic solvents.[7,14] In line with the growing environmental awareness, the academic community has been exploring ecofriendly alternatives for detecting HAA. Hybrid materials containing coordination compounds in a polymer matrix of chitosan, a natural biodegradable polymer, have been proposed[15-21] as electrochemical, fluorescence, and colorimetric sensors for several substances including HAA. The unique features resultant from the combination of different compounds in a hybrid material

*e-mail: izaura@dqoi.ufc.br
Editor handled this article: Célia M. Ronconi (Associate)

may be tailored to meet specific application requirements. In this context, the incorporation of pentacyanoferrate(II) complexes in chitosan films has been used for detecting heavy metals and HAA like molecules.[16,22-24] In addition, chitosan films are typically transparent allowing the use of spectrophotometric methods. In fact, the approach used for the recognition of pyrazine (pz),[16] a reference molecule used to mimic HAA, was based on the color change resultant from the substitution reaction shown in Figure 1.

Hunger, a pressing and urgent global issue, demands political efforts for equitable income distribution and development of sustainable technologies to guarantee safe food supply while mitigating climate change effects. In this regard, chitosan has been widely used to make biodegradable packaging materials in the food industry. However, the propensity for hydrolysis reactions is a disadvantage because it affects the mechanical properties and diminishes the robustness of the material. On the other hand, the positive charge density of chitosan and its ability to interact with other compounds provide the possibility of robustness improvement making this polymer a valuable organic support material indeed. The numerous ways that chitosan can interact with different substances provide a significant advantage for this biopolymer in practical applications.[25] Pretreatment or the incorporation of materials into the biopolymer support can enhance the mechanical properties like tensile strength and flexibility, which are essential for packaging.[25-27] Several approaches have been adopted to improve the mechanical properties of chitosan-based films. A recent review[28] on the use of chitosan for food packaging applications highlights the mixing with materials like polylactic acid,[27] polysaccharides,[29] and inorganic materials,[30] among others, to ensure that the resulting packaging can withstand stresses, transportation and preservation as well.

The main goal of this work is to take a step further in respect to the previous study carried out by our group,[16] both with regard to the preparation of the chitosan films and the incorporation of the aquapentacyanoferrate(II) complex. As result, more robust hybrid materials were produced containing a relatively higher amount of the inorganic compound thus leading to better results of detection of HAA like molecule. To study the detection ability at this time, we chose quinoxaline (IQx, structure shown in Figure 1) because of the molecular skeleton that is very similar to most HAA species.

Experimental

Chemicals

All reagents used were obtained from commercial sources without previous purification. Chitosan (degree of deacetylation 75-85%), quinoxaline (≥ 99%), trifluoroacetic acid (99%), sulfuric acid (95-98%), histidine (≥ 98%), methionine (≥ 99%), and tryptophan (≥ 99%) were obtained from Sigma-Aldrich (São Paulo, Brazil). Sodium nitroprusside, $Na_2[Fe(CN)_5(NO)].2H_2O$ (99%) and acetic acid (≥ 99.7%) were obtained, respectively, from Merck (São Paulo, Brazil) and Tedia (Rio de Janeiro, Brazil). H_2O_2 (35%) was purchased from Neon (Suzano, Brazil), and NaOH (> 98%), $MgSO_4$ (> 98%), NaCl (> 98%), ethyl acetate (> 98%), and ethanol (95%) were obtained from Synth (São Paulo, Brazil). All other organic solvents used were of comparable analytical grade or purity. Aqueous solutions were prepared using ultrapure water (Millipore Co., Bedford, USA) with a resistance of 18 MΩ cm at 25 °C.

Apparatus

Chitosan films were characterized by electronic spectroscopy in the ultraviolet and visible (UV-Vis) regions, scanning electron microscopy (SEM), water contact angle, and atomic absorption spectrometry (AAS) using, respectively, the following equipments Varian Cary 5000 UV-Vis-NIR (Palo Alto, USA), Quanta 450 FEG-FEI (Graz, Austria) operating with an acceleration voltage of 5 kV, contact angle instrument model GBX Instrumentation Scientific (Dublin, Ireland) with a drop of distilled water, and Varian AA240FS fast sequential atomic absorption spectrometer (Palo Alto, USA).

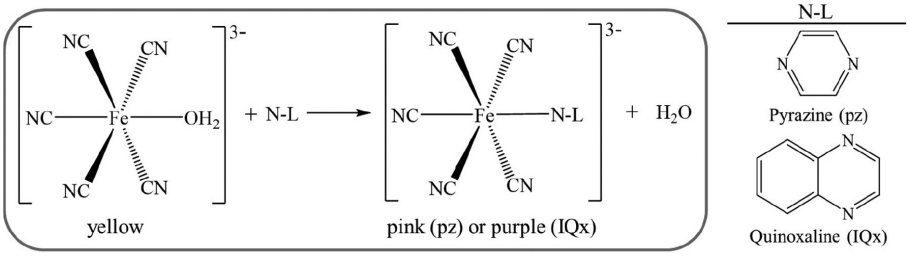

Figure 1. Illustrative representation of a substitution reaction showing the replacement of a water molecule of $[Fe(CN)_5(OH_2)]^{3-}$ by a *N*-heterocyclic ligand (*N*-L) leading to color change from yellow to pink (pz) or purple (IQx).

Synthesis of $[Fe(CN)_5(OH_2)]^{3-}$

The starting complex $[Fe(CN)_5(NH_3)]^{3-}$ was synthesized following the previously reported procedure.[31] The *in situ* preparation of $[Fe(CN)_5(OH_2)]^{3-}$ was conducted by dissolving 0.625 mg of $[Fe(CN)_5(NH_3)]^{3-}$ in 10 mL of water, resulting in a solution with a final concentration of 2×10^{-4} mol L^{-1}.

Preparation of hybrid materials

Chitosan films

The chitosan films were produced using a 2% (m/v) chitosan solution, prepared by dissolving 1 g of chitosan powder in a 1% (v/v) acetic acid solution, as previously reported.[16] An aliquot of 1 mL of the prepared chitosan solution was dropped onto plastic Petri dishes and stored in a sealed container with silica gel for 48 h for slow drying resulting in circular films with a diameter of 2.5 cm. The produced CS films were subjected to a pretreatment as follows: immersion in ethanol (EtOH) for 24 h and subsequently in a 1.0×10^{-3} mol L^{-1} solution of NaOH (2 s).

Adsorption of $[Fe(CN)_5(OH_2)]^{3-}$ into chitosan films

In this work, the modification of the CS films followed a protocol different from the previous one published by our group[16] to avoid mixing the solutions of the chitosan and complex. At this time, the CS films pretreated with EtOH and NaOH were immersed in 10 mL of a 2×10^{-4} mol L^{-1} aqueous solution of $[Fe(CN)_5(OH_2)]^{3-}$ (for different times and temperatures) producing the CS-Fe hybrid material.

Quantification of $[Fe(CN)_5(OH_2)]^{3-}$ adsorbed into the chitosan films

The amount of the $[Fe(CN)_5(OH_2)]^{3-}$ complex adsorbed in the chitosan matrix was evaluated by atomic absorption spectrometry and UV-Vis spectroscopy. For the atomic absorption analyses, the samples were previously mixed with 1.0 mL of concentrated H_2SO_4 and 0.5 mL of H_2O_2 (29% v/v) and maintained at 25 °C until complete dissolution (ca. 30 min). The produced solution was diluted to 10.0 mL and the pH was adjusted to 3.0 by adding NaOH solution (4.0 mol L^{-1}). After that, the solution was diluted again to 25.0 mL and the atomic absorption measurements were done. For the UV-Vis measurements (Figure S1, presented in Supplementary Information (SI) section), a calibration curve (Figure S2, SI section) was previously constructed following the intensity of the band at 230 nm, assigned[32] to metal-to-ligand charge-transfer (MLCT) transition from the $d\pi$ orbitals of Fe^{II} to π^* orbitals of CN^- of the $[Fe(CN)_5(OH_2)]^{3-}$ ion complex. The calibration curve allowed the estimation of the limits of detection (LOD) and quantification (LOQ) as 5.69 and 10.78 μmol L^{-1}, respectively. The method applied for determining LOD and LOQ is described in the SI section (equations S1 and S2). The quantification was achieved by using the difference between the concentrations of the complex before and after the adsorption process that was performed at 15, 20, 25, 35 and 40 °C. For the spectra acquisition, 2.0 mL aliquots were taken from the working solution at intervals of 5 min. After each spectrum registration, the aliquot was turned back to the working solution to avoid concentration variations.

Desorption experiments were also carried out to evaluate the percentage of leaching of the complex from the chitosan matrix. Typically, 19.0 mg of the CS-Fe film were added to a Falcon® tube containing 10.0 mL of ultrapure water and stirred for 60 min at 25 °C. The amount of $[Fe(CN)_5(OH_2)]^{3-}$ desorbed was indirectly determined by UV-Vis following the band at 230 nm. The spectra of 2.0 mL aliquots were acquired at intervals of 10 min with the samples being returned to the working solution to avoid concentration variations.

Both the adsorption and desorption experiments were carried out in triplicate.

Application of the hybrid material as sensor

Quinoxaline control sample

Quinoxaline (IQx) was used in this study to mimic HAA molecules. As a general protocol, 19.0 mg of the CS-Fe film were immersed in aqueous solutions of IQx and the interaction was monitored by UV-Vis electronic spectroscopy following the band at 535 nm (Figure S3, SI section). A calibration curve (Figure S4, SI section) was constructed for the determination of LOD (4.46 mmol L^{-1}) and LOQ (14.9 mmol L^{-1}). All these experiments were performed in triplicate.

Real samples

Frozen hamburger meat purchased in a local market was used to prepare the real samples in this work. The samples went through a pretreatment adapted from a protocol reported for chromatographic analysis of meat.[33] A roasted meat sample of 2.0 g was cut with a knife, spiked with 0.18 g of quinoxaline, and dispersed in 14 mL of ultrapure water, vortexed for 1 min and ultrasonicated for 30 min. Then, 15 mL of ethyl acetate was added, and the tube was vortexed for 1 min followed by the addition of $MgSO_4$ (3.0 g) and NaCl (1.0 g) and, again, vortexed for 1 min and centrifugation at 4000 rpm (25 °C) for 5 min. After formation of two phases (Figure S5, blue cap, SI section), the organic phase

containing IQx (Figure S5, red cap, SI section) was separated for incubating the hybrid materials.

Interference studies

Because of the very likely presence in the meat samples of methionine, histidine, and tryptophan, which could coordinate to Fe^{II}, UV-Vis experiments were performed to evaluate possible interferences. For the spectra acquisition, the hybrid materials were sequentially immersed (one at a time) in the amino acid aqueous solution (0.10 mol L^{-1} of methionine or histidine, and 0.01 mol L^{-1} of tryptophan) and in a 0.10 mol L^{-1} solution of IQx for 10 min. After dryness, the UV-Vis spectra were acquired using a Varian Cary spectrophotometer equipped with a solid sample holder. Same procedure was applied for the bicomponent (0.10 mol L^{-1} of His and 0.01 mol L^{-1} of Trp) and tricomponent (0.10 mol L^{-1} of His, 0.01 mol L^{-1} of Trp, and 0.10 mol L^{-1} of IQx) mixtures.

Results and Discussion

Lately, the interest in hybrid materials that include biopolymers for use in analyses related to food safety has increased due to environmental awareness, among other concerns. The idea in this work is to present a hybrid material composed of a chitosan film incorporated with molecules of aquapentacyanoferrate(II) complex (CS-Fe), which is the active moiety for the detection of quinoxaline (IQx), a reference compound to mimic heterocyclic aromatic amines (HAA). Aiming to produce more robust materials, we present here a modified protocol for both the chitosan film preparation and the adsorption of the complex into the polymer matrix.

Chitosan film preparation and adsorption of $[Fe(CN)_5(OH_2)]^{3-}$

Chitosan film preparation

At first, circular chitosan films of 2.5 cm diameter were produced from a 2% (m/v) chitosan solution following a traditional protocol described in the literature.[16] In a second step, aiming to improve the mechanical properties such as strength and flexibility, the films were immersed in EtOH for 24 h leading to dehydration and formation of hydrogen bonds between the chitosan chains implying an increase of resistance against deformation and swelling.[34-36] A third and final step was applied to the films to avoid swelling and expanding due to the absorption of water and/or anionic compounds. In fact, the natural chitosan polymer is solubilized in a 1% (v/v) acetic acid solution that results in cationic properties thus facilitating the absorption of water and anionic compounds. Because of that, the third step was a partial neutralization reaction with a 1.0 mmol L^{-1} solution of NaOH (pH 11). In the end, EtOH and NaOH act in tandem to improve the mechanical properties of the chitosan film. Figure 2 shows the micrographs (SEM) obtained at each step of the chitosan film preparation.

The grooves observed in the micrograph shown in Figure 2a are associated to the plastic Petri dish used as support during dryness. After immersion in EtOH for 24 h, a rougher surface (Figure 2b) is observed indicating an increase of the intermolecular interactions and compactness consistent with the formation of hydrogen bonds. The image obtained after the immersion in NaOH (Figure 2c), although showing small cracks, indicates the robustness of the film in respect to those that did not go through the steps 2 and 3. In fact, this stability improvement against moisture absorption has been reported[36,37] for chitosan films. Accordingly, the neutralization with NaOH followed by ethanol washing removes part of the water and acetic acid molecules resulting in a annealed polymorph chitosan film that is more compact because of additional inter-chain hydrogen bonds.[36,38,39]

It is worth mentioning that the untreated chitosan film exhibits swelling after a brief exposure to air humidity and undergoes oxidative degradation when in contact with aqueous acidic solution. In contrast, the film treated with EtOH and NaOH remains intact for over 60 days in aqueous solutions and shows resistance to degradation in

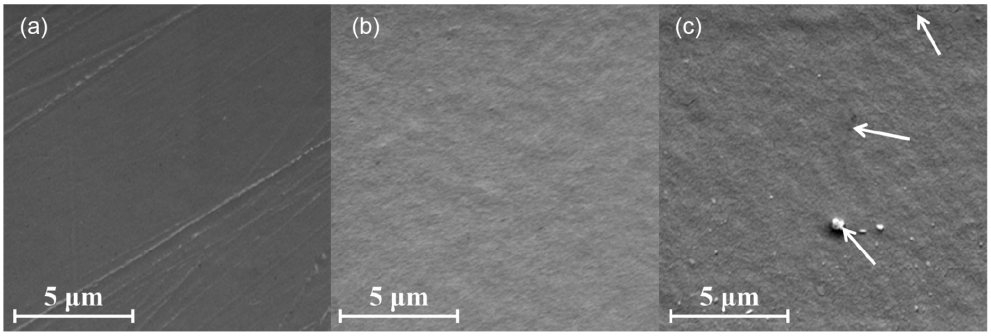

Figure 2. Micrographs (SEM) obtained for the as-prepared CS film (a), and after sequential immersions in EtOH for 24 h (b) and in a 1.0 mmol L^{-1} solution of NaOH for 2 s (c).

acidic media, being oxidized solely by piranha solution ($1H_2O_2$:$3H_2SO_4$).

Adsorption of $[Fe(CN)_5(OH_2)]^{3-}$ in chitosan films

Differently from the previous paper published by our group,[16] the modification of the chitosan films with the aquapentacyanoferrate(II) complex in this study followed another protocol aimed at improving the stability of the final hybrid materials.[34] Instead of mixing the solutions of chitosan and complex, the CS films previously treated with EtOH and NaOH were immersed in a 2×10^{-4} mol L^{-1} aqueous solution of $[Fe(CN)_5(OH_2)]^{3-}$ varying the temperature and the immersion time. The adsorption of $[Fe(CN)_5(OH_2)]^{3-}$ in the CS films was monitored by UV-Vis spectroscopy following the band at 230 nm (Figure S1a), assigned[32] to the MLCT transition from the dπ orbitals of Fe^{II} to the π* orbitals of the CN^- ligands. Figure 3a shows the decay of the absorbance at 230 nm as function of the immersion time. The spectra from which the points of the curve were extracted, were registered at intervals of 5 min from 2.0 mL aliquots taken from the working solution.

As can be ascertained from the plot shown in Figure 3a, the decay of the absorbance indicates that the concentration of the complex in solution decreases due to the adsorption in the CS film thus producing the CS-Fe hybrid material. Considering the experimental conditions, an immersion time of 30 min is enough to reach saturation of the CS film at 25 °C. The spectroscopic monitoring following the intensity of the band at 230 nm was also applied to evaluate the release of the complex from the film (Figure S1b). For that, the CS-Fe film was immersed in water and 2.0 mL aliquots were taken at intervals of 10 min for the spectra acquisition. The percentage of the ratio of the desorbed mass of the complex to the mass of the CS film (Figure S1b, inset) increases fast in the first 10 min and very slowly up to 50 min presenting a total variation of less than 5%. This result indicates that the amount of complex released from the chitosan film is negligible.

The micrograph (Figure 3b) obtained after the adsorption of $[Fe(CN)_5(OH_2)]^{3-}$ in the CS film (CS-Fe) presented no difference in respect to that shown in Figure 2c, meaning the molecules of the complex do not lead to topographic changes.

The adsorption process of $[Fe(CN)_5(OH_2)]^{3-}$ in the CS film is temperature-dependent and displays an endothermic behavior (Figure S6, see SI section). As observed for the adsorption of methyl orange dye,[40] higher temperatures might induce the increase of the pore sizes of the chitosan film thus facilitating the incorporation of $[Fe(CN)_5(OH_2)]^{3-}$.

Atomic absorption spectrometry (AAS) was also used for quantifying the $[Fe(CN)_5(OH_2)]^{3-}$ ion complex adsorbed in the CS films as a validating tool. Table 1 shows the quantification data obtained by UV-Vis and AAS.

Table 1. Amount of $[Fe(CN)_5(OH_2)]^{3-}$ adsorbed *per* gram of chitosan film as determined by UV-Vis and AAS techniques

Sample	Amount / (μmol g^{-1})	
	UV-Vis	AAS
1	51.63	58.31
2	55.96	57.80
3	54.40	56.29
Mean value ± standard deviation	54.00 ± 2.19	57.47 ± 1.05
CV / %	4.06	1.83

UV-Vis: ultraviolet and visible; AAS: atomic absorption spectrometry; CV: coefficient of variation.

Coefficient of variation of less than 5% among the triplicate UV-Vis and AAS experiments (Table 1) indicate the acquisition of reliable data[41] that could be used for

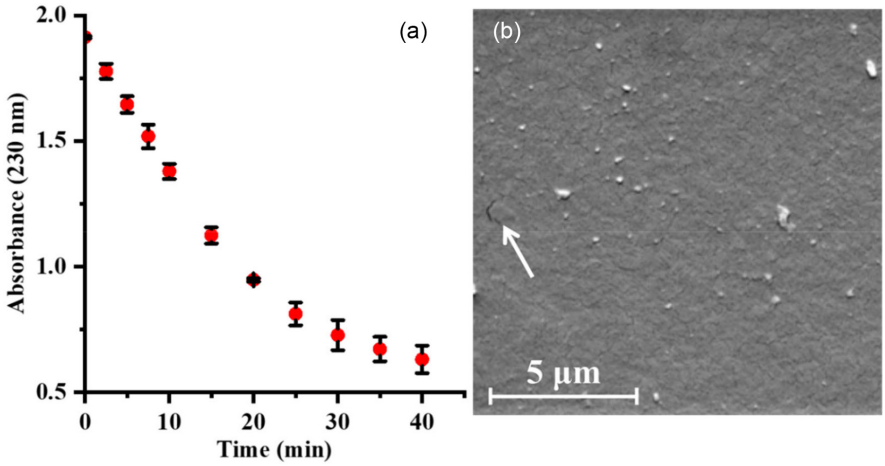

Figure 3. (a) Decay monitoring of the band at 230 nm during the adsorption process of $[Fe(CN)_5(OH_2)]^{3-}$ (initial concentration: 2×10^{-4} mol L^{-1}) in the CS film at 25 °C, and (b) micrograph (SEM) of the CS-Fe film.

the quantification of $[Fe(CN)_5(OH_2)]^{3-}$ adsorbed in the CS films, which was found to be 54.00 ± 2.19 μmol g^{-1} at 25 °C. Such value is more than twice as those previously reported[16,24] for the adsorption of pentacyanoferrate(II) complexes in chitosan (ca. 20 μmol g^{-1}). We hypothesize this increase in the adsorption capacity is due to (*i*) the pretreatment of the CS film with EtOH and NaOH; and (*ii*) the change in the adsorption protocol. In this work, the CS films were immersed in the complex solution instead of having the solutions of the complex and chitosan mixed to obtain the films.

Water contact angle (WCA) measurements

To determine the swelling degree (SD) of the CS films before and after the adsorption of the complex, water contact angle (θ) measurements were performed, and the results are shown in Figure 4a.

Values of θ higher and lower than 90° define hydrophobic and hydrophilic surfaces, respectively.[42] During the preparation of the CS film, the water contact angle virtually does not change after immersion in EtOH (from 76.2 to 78.5°). However, the treatment with NaOH strongly affects the property of the film increasing its hydrophilicity (θ = 50.7°). This result is assigned to the presence of the $–NH_2$ and –OH groups on the surface of the polymer that facilitates the formation of hydrogen bonds between the water molecules (from the water droplet) and chitosan allowing adsorption rather than absorption of water. Such phenomenon contributes to the hydrophilic nature of the film and its interaction with water. Upon the adsorption of $[Fe(CN)_5(OH_2)]^{3-}$, the contact angle increases again (θ = 81.1°) very likely because of the replacement of the water molecules of the CS film by those of the complex.

To provide a more comprehensive understanding of these effects, the SD of the CS film was evaluated at each stage of the treatment, following equation 1:[43]

$$SD = \frac{W_t - W_0}{W_0} \quad (1)$$

where W_0 and W_t are, respectively, the weight of the film before and after immersion in water. The obtained values are plotted in Figures 4b and 4c that present a zoom in for the data obtained after immersion of the CS film in EtOH and NaOH. Accordingly, after immersion in EtOH and NaOH, a meaningful decrease in the swelling degree of the CS film is observed, dropping from 80 to ca. 0.8 (after 60 s) thus indicating that the capacity of the film to absorb water is drastically diminished. This behavior is associated with the improvement of the film resistance against the absorption of water due to the pretreatment with EtOH and NaOH.

Application of the hybrid material Cs-Fe in the detection of IQx

The produced CS-Fe films showed a meaningful color change when exposed to IQx solutions, going from pale yellow to purple due to the replacement of one water molecule by IQx in the coordination sphere of the iron complex, as shown in Figure 1. The new complex formed

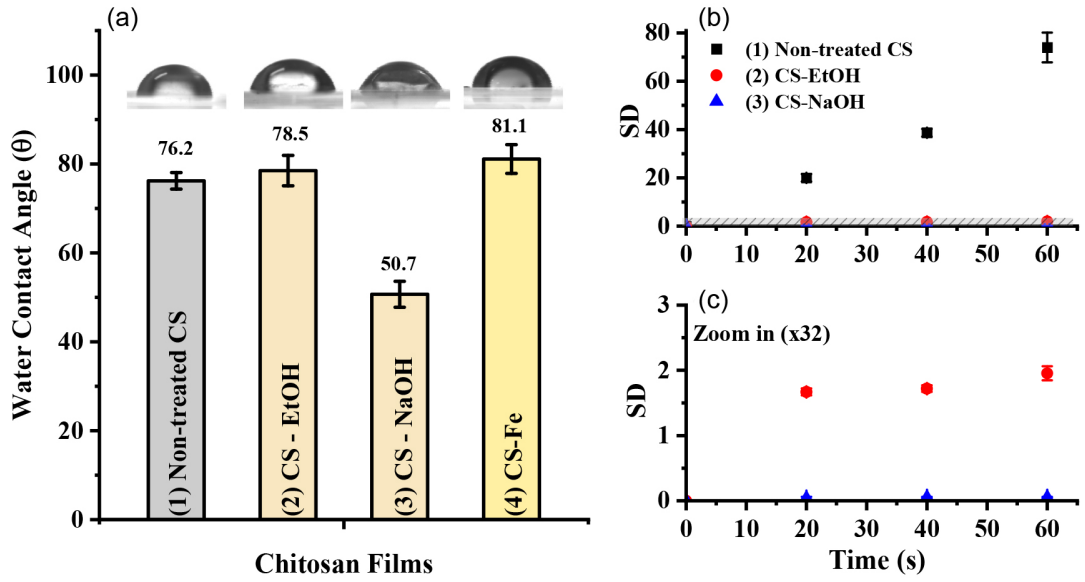

Figure 4. (a) Bar graph showing the values of water contact angle (θ) obtained for the CS film after each step preparation and adsorption of $[Fe(CN)_5(OH_2)]^{3-}$ (CS-Fe); (b) swelling degree (SD) for the non-treated CS film (■) and after immersion in EtOH (●) and NaOH (▲); (c) zoom in (32×) of the curves obtained for the CS film after immersion in EtOH (●) and NaOH (▲).

within the chitosan matrix, $[Fe(CN)_5(IQx)]^{3-}$, presents a MLCT transition with maximum at 535 nm (Figure S3a) thus explaining the purple color. The intensity of this band was monitored as a function of the immersion time of the CS-Fe film in the IQx solution (Figure S3b) indicating a fast ligand exchange with no further variation for immersion times longer than 10 min.

The response of the CS-Fe film to IQx in a real sample was studied in suspensions of hamburger meat spiked with IQx. Figure 5 shows the UV-Vis spectra and photographs obtained for the CS-Fe film before and after immersion in the meat suspension spiked with IQx.

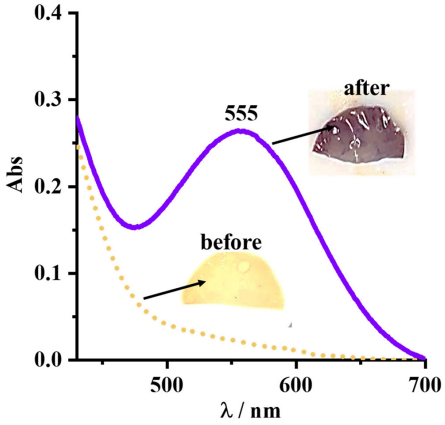

Figure 5. UV-Vis spectra and photographs obtained for the CS-Fe films before (yellow dotted line) and after (purple solid line) 10 min of immersion in the meat suspension spiked with IQx.

The color difference observed in the photographs of the CS-Fe films before (yellow) and after (purple) exposure to the meat suspension spiked with IQx proves, qualitatively, the effectiveness of the visible detection of IQx by the hybrid material. Indeed, the meat suspension presents a pale brown color (Figure S5) meaning that the color change of the CS-Fe film must be associated with the coordination of IQx to the iron metal center. As a matter of fact, the UV-Vis spectrum acquired for the CS-Fe film after immersion in the suspension of the hamburger meat spiked with IQx (purple line in Figure 5) presents the same profile as that obtained after immersion in pure IQx solution (Figure S3a). Applying the maximum absorbance value of the spectrum shown in Figure 5 (purple line) to the calibration curve of IQx (Figure S4), a real concentration of 0.089 mol L^{-1} was found for IQx. This value is very close to the expected value (0.092 mol L^{-1}) due to the addition of 0.18 g of IQx in 15 mL of solution. This result hints that the CS-Fe film is capable of selectively, and quantitatively, detecting IQx in a real sample despite the presence of possible interference compounds as will be discussed later. In respect to the spectrum obtained after exposure to a pure IQx solution (Figure S6a), there is a red shift from 535 to 555 nm. This shift is indeed expected since the band at 555 nm is assigned to a MLCT charge-transfer transition which is strongly affected by the solvent nature. Upon the meat dissolution, the presence of organic matter alters the chemical nature of the medium changing the dipole interactions between the solvent and the excited state and, as consequence, the energy of the transition.

Interference study

A few nutrients found in meat contain amino acids such as methionine (Met), tryptophan (Trp) and histidine (His) that may coordinate to iron(II) interfering in the detection process of HAA type molecules, such as IQx. To evaluate the interference of these species, UV-Vis spectra of the Cs-Fe films were acquired after immersion in IQx solution upon exposure to solutions of Met, Trp, and His. The obtained spectra are shown in Figure 6.

The spectra obtained for CS-Fe after immersion in IQx solution upon exposure to Met and Trp (purple lines in Figures 6a and 6b) indicate that these amino acids do not interfere in detecting IQx. It should be mentioned that Trp might coordinate to iron(II) through a substitution reaction giving rise to two absorptions at 521 and 705 nm (Figure 6b) assigned to MLCT transitions, $n\pi^*(Trp) \leftarrow d\pi(Fe^{2+})$. The coordination of Trp moiety, however, seems to be labile since this species is promptly replaced by IQx as can be ascertained from the recovery of the spectral profile assigned to the $[Fe(CN)_5(IQx)]^{3-}$ complex (band at 545 nm in the purple spectrum in Figure 6b). On the other hand, the coordination of His to the iron metal center is strong enough to not allow the subsequent replacement by IQx. As shown in Figure 6c, the typical spectrum of the CS-Fe film containing IQx, $[Fe(CN)_5(IQx)]^{3-}$ (Figure S3), is no longer obtained after exposure to the His solution. Rather, a new band at 520 nm is observed being associated with a MLCT transition to His, $n\pi^*(His) \leftarrow d\pi(Fe^{2+})$.

Figure 7 shows the spectra obtained after different immersion times of the CS-Fe film in a tricomponent mixture containing IQx and the amino acids that have experienced any interaction with the metal center, i.e., Trp and His.

After 30 s of immersion in the tricomponent mixture, the obtained spectrum (red line) shows a band with maximum at 545 nm indicating the formation of $[Fe(CN)_5(IQx)]^{3-}$ within the chitosan matrix. The intensity of this band reaches its maximum after 60 s (blue line) and gradually decreases thereafter (gray lines). After about 150 s, a new band at around 520 nm appears suggesting the coordination of His. As the immersion time increases, however, the intensity of this band significantly decreases, as evidenced by the last two spectra recorded after 300 and 330 s, magenta

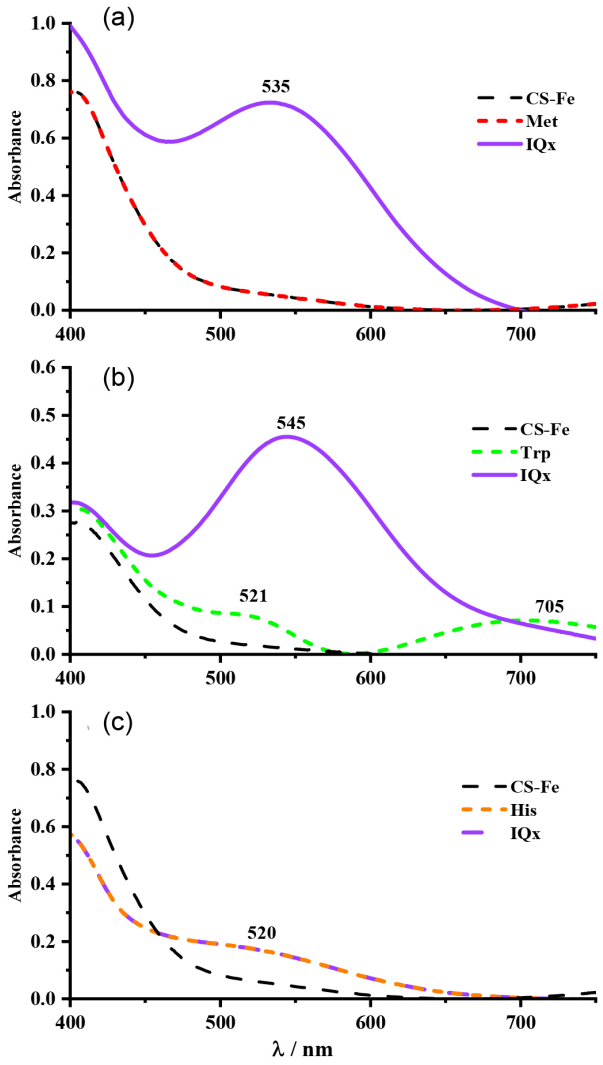

Figure 6. UV-Vis spectra of the CS-Fe films after 10 min of immersion in solutions of (a) Met (···), (b) Trp (···), and (c) His (···). The purple line (—) in all figures stands for the spectra obtained for the CS-Fe films after 10 min of immersion in IQx solution upon exposure to amino acid solutions. The spectra were acquired in the following final concentrations: 0.01 mol L^{-1} for Trp and 0.1 mol L^{-1} for IQx, Met, and His.

and purple lines, respectively. This result indicates the spectrophotometric detection of IQx in solution by CS-Fe films should be carried out within a maximum exposure time of 60 s to avoid interference from histidine. It should be emphasized, however, that histidine, although considered in this work as a potential interfering substance, is a common constituent of meat proteins and is rarely found in free form in solution. Therefore, it might not be considered as a real barrier to the use of the CS-Fe film as a colorimetric sensor for HAA type molecules.

Conclusions

We presented in this work a modified protocol for producing a hybrid material based on a transparent

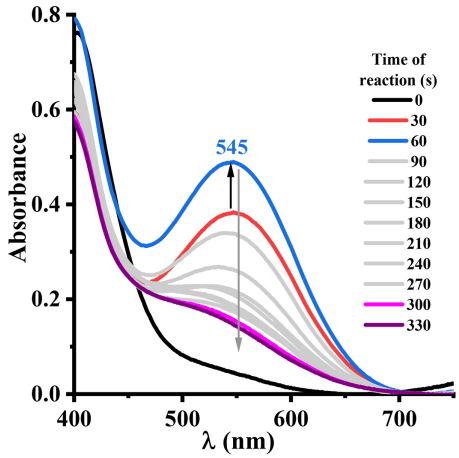

Figure 7. UV-Vis spectra of the CS-Fe film after different immersion times in a tricomponent mixture containing 0.10 mol L^{-1} of His and IQx, and 0.01 mol L^{-1} of Trp. Red and blue lines indicate the first and second collected spectra, respectively, while magenta (300 s) and purple (330 s) lines stand for the last two spectra.

film of chitosan (CS), a natural polymer, containing $[Fe(CN)_5(OH_2)]^{3-}$ (CS-Fe). The immersion of CS films in EtOH and NaOH solutions, which lead to dehydration and formation of hydrogen bonds among chitosan chains, enhanced resistance against deformation and swelling, as demonstrated by scanning electron microscopy and water contact angle measurements. In the proposed protocol, EtOH and NaOH showed to act in tandem to improve the mechanical properties of the CS film in addition to having more than doubled the adsorption capacity for $[Fe(CN)_5(OH_2)]^{3-}$. Electronic spectroscopy and atomic absorption spectrometry were used to determine the amount of $[Fe(CN)_5(OH_2)]^{3-}$ adsorbed within the polymer matrix giving a mean value of 54.00 ± 2.19 μmol *per* gram of CS film at 25 °C. The CS-Fe hybrid material is sensitive to the presence of HAAs like molecules, such as quinoxaline (IQx), due to the substitution reaction of water that led to color change from pale yellow (CS-Fe) to purple (in the case of IQx). Accordingly, the capacity of the CS-Fe film in detecting IQx was studied by electronic spectroscopy following the band at 535 nm assigned to the charge transfer transition from Fe^{II} to IQx in the $[Fe(CN)_5(IQx)]^{3-}$ complex within the polymer matrix. The study in real samples was performed in suspensions of hamburger meat spiked with IQx and showed the CS-Fe film is capable to selectively detect IQx even in presence of the most likely interfering amino acids, i.e., methionine, tryptophan, and histidine.

Supplementary Information

Supplementary data (spectroscopic monitoring of the iron complex adsorption/desorption into/from the chitosan (CS) film; calibration curve for quantifying the

adsorbed iron complex in CS films; statistical treatment of the quantification data of the iron complex adsorption as obtained by UV-Vis spectroscopy and atomic absorption spectrometry; spectroscopic study of the hybrid material after exposure to quinoxaline (IQx) solution; calibration curve for quantifying IQx in the hybrid material; photographs of the suspensions of the real samples; analysis of the iron complex adsorption in CS film at different temperatures) are available free of charge at http://jbcs.sbq.org.br as PDF file.

Acknowledgments

This study was financed in part by Coordenação de Aperfeiçoamento de Pessoal de Nível Superior - Brasil (CAPES), finance code 001. E. Longhinotti (309105/2021-8) and I. C. N. Diogenes (311274/2020-0) are thankful to Conselho Nacional de Desenvolvimento Científico e Tecnológico (CNPq) for the grants. The authors are thankful to Coordenação de Aperfeiçoamento de Pessoal de Nível Superior (CAPES)/Programa de Extensão Universitária (PROEX) 23038.011210/2020-53 and Financiadora de Estudos e Projetos (FINEP, CV. 01.22.0174.00) for financial support.

References

1. Andrade, G. C.; Gombi-Vaca, M. F.; Louzada, M.; Azeredo, C. M.; Levy, R. B.; *Public Health Nutr.* **2020**, *23*, 1041. [Crossref]
2. Isaksen, I. M.; Dankel, S. N.; *Clin. Nutr.* **2023**, *42*, 919. [Crossref]
3. Taş, N. G.; Kocadağlı, T.; Gökmen, V.; *Curr. Opin. Food Sci.* **2022**, *47*, 100876. [Crossref]
4. Cordova, R.; Viallon, V.; Fontvieille, E.; Peruchet-Noray, L.; Jansana, A.; Wagner, K. H.; Kyrø, C.; Tjønneland, A.; Katzke, V.; Bajracharya, R.; Schulze, M. B.; Masala, G.; Sieri, S.; Panico, S.; Ricceri, F.; Tumino, R.; Boer, J. M. A.; Verschurenm, W. V. M.; van der Schouw, V. T.; Jakszyn, P.; Redondo-Sánchez, D.; Amiano, P.; Huertas, J. M.; Guevaras, M.; Borné, Y.; Sonestedt, E.; Tsilidis, E. K.; Millett, K.; Heath, A. K.; Aglago, E. K.; Aune, D.; Gunter, M. J.; Ferrari, P.; Huybrechts, I.; Freisling, H.; *Lancet Reg. Health - Eur.* **2023**, *35*, 100771. [Crossref]
5. Sugimura, T.; Wakabayashi, K.; Nakagama, H.; Nagao, M.; *Cancer Sci.* **2004**, *95*, 290. [Crossref]
6. Zaoui, M.; Louadj, L.; Ferrand, N.; Nehme, R.; Sabbah, M.; Abdennebi-Najar, L.; *Food Chem. Toxicol.* **2024**, *185*, 114454. [Crossref]
7. Oz, E.; Aoudeh, E.; Murkovic, M.; Toldra, F.; Gomez-Zavaglia, A.; Brennan, C.; Proestos, C.; Zeng, M.; Oz, F.; *Meat Sci.* **2023**, *205*, 109312. [Crossref]
8. International Agency for Research on Cancer (IARC); *World Cancer Reports 2014*; IARC: Lyon, France, 2014. [Link] acessed in December 2024
9. Jägerstad, M.; Skog, K.; Arvidsson, P.; Solyakov, A.; *Z. Lebensm. -Unters. Forsch.* **1998**, *207*, 419. [Crossref]
10. Barzegar, F.; Kamankesh, M.; Mohammadi, A.; *Food Chem.* **2019**, *280*, 240. [Crossref]
11. Zhang, H.; Lv, X.; Su, W.; Chen, B. H.; Lai, Y. W.; Xie, R.; Lin, Q.; Chen, L.; Cao, H.; *Food Chem.* **2024**, *446*, 138760. [Crossref]
12. Mansour, S. T.; Ibrahim, H.; Zhang, J.; Farag, M. A.; *Food Chem.* **2025**, *464*, 141736. [Crossref]
13. Santé-Lhoutellier, V.; Astruc, T.; Marinova, P.; Greve, E.; Gatellier, P.; *J. Agric. Food Chem.* **2008**, *56*, 1488. [Crossref]
14. Sontag, G.; Pinto, M. I.; Noronha, J. P.; Burrows, H. D.; *J. Agric. Food Chem.* **2019**, *67*, 4113. [Crossref]
15. Zhang, B.; Li, C.; Jia, W.; Zhang, W.; Huang, N.; Sheng, W.; Wang, S.; *Sens. Actuators, B* **2021**, *337*, 129759. [Crossref]
16. Silva, M. A. S.; Abreu, D. S.; Costa, L. A.; Aguiar, N. A.; Paulo, T. F.; Longhinotti, E.; Diógenes, I. C. N.; *J. Agric. Food Chem.* **2017**, *65*, 1387. [Crossref]
17. Huang, T. W.; Lu, H. T.; Ho, Y. C.; Lu, K. Y.; Wang, P.; Mi, F. L.; *Mater. Sci. Eng., C* **2021**, *118*, 111396. [Crossref]
18. Delolo, F. G.; Rodrigues, C.; Silva, M. M.; Dinelli, L. R.; Delling, F. N.; Zukerman-Schpector, J.; Batista, A. A.; *J. Braz. Chem. Soc.* **2014**, *25*, 550. [Crossref]
19. Laranjo, M. T.; Morawski, F. M.; Dias, S. L. P.; Benvenutti, E. V.; Arenas, L. T.; Costa, T. M. H.; *J. Braz. Chem. Soc.* **2019**, *30*, 2660. [Crossref]
20. Silva, J. O. S.; Granja, H. S.; Santos, J. F.; Freitas, L. S.; Sussuchi, E. M.; *J. Braz. Chem. Soc.* **2024**, *35*, e-20230143. [Crossref]
21. Teixeira, L. S.; Carvalho, S. Y. B.; Santos, A. C.; Borges, M. M. C.; Vieira, S. S.; Borges, K. B.; Guimarães, L. G. L.; *J. Braz. Chem. Soc.* **2024**, *35*, e-20240048. [Crossref]
22. Bratskaya, S. Y.; Zheleznov, V. V.; Privar, Y. O.; Mehaev, A. V.; Pestov, A. V.; *Sep. Sci. Technol.* **2016**, *51*, 594. [Crossref]
23. Bratskaya, S. Y.; Privar, Y. O.; Korjakova, O. V.; Mechaev, A. V.; Pestov, A. V.; *Polym. Eng. Sci.* **2014**, *54*, 2392. [Crossref]
24. Bratskaya, S. Y.; Zheleznov, V. V.; Privar, Y. O.; Mechaev, A. V.; Zub, Y. L.; Pestov, A. V.; *Colloids Surf., A* **2014**, *460*, 145. [Crossref]
25. Das, P. P.; Prathapan, R.; Ng, K. W.; *Biomater. Adv.* **2024**, *164*, 213988. [Crossref]
26. Yuan, J.; Li, J.; Huang, J.; Wu, H.; Tan, J.; Li, H.; *Ind. Crops Prod.* **2024**, *222*, 119641. [Crossref]
27. Nambiar, R. B.; Sellamuthu, P. S.; Perumal, A. B.; Sadiku, E. R.; Adeyeye, O. A. In *Green Biopolymers and their Nanocomposites*; Gnanasekaran, D., ed.; Springer: Singapore, 2019.

28. Barik, M.; BhagyaRaj, G. V. S.; Dash, K. K.; Shams, R.; *J. Agric. Food Res.* **2024**, *16*, 101164. [Crossref]
29. Lima, M. M.; Carneiro, L. C.; Bianchini, D.; Dias, A. R. G.; Zavareze, E. R.; Prentice, C.; Moreira, A. S.; *J. Food Sci.* **2017**, *82*, 698. [Crossref]
30. Oghani, F. Z.; Tahvildari, K.; Nozari, M.; *J. Inorg. Organomet. Polym. Mater.* **2021**, *31*, 43. [Crossref]
31. Brauer, G.; *Handbook of Preparative Inorganic Chemistry*, vol. 1, 2nd ed.; Elsevier: London, UK, 1963. [Crossref]
32. Toma, H. E.; Malin, J. M.; *Inorg. Chem.* **1973**, *12*, 1039. [Crossref]
33. Jian, S. H.; Yeh, P. J.; Wang, C. H.; Chen, H. C.; Chen, S. F.; *J. Food Drug Anal.* **2019**, *27*, 595. [Crossref]
34. Lu, H.; Wang, W.; Wang, A.; *RSC Adv.* **2015**, *5*, 17775. [Crossref]
35. Mikhailov, G. P.; Lazarev, V. V.; *Russ. J. Phys. Chem. A* **2016**, *90*, 1367. [Crossref]
36. He, Q.; Ao, Q.; Gong, Y.; Zhang, X.; *J. Mater. Sci.: Mater. Med.* **2011**, *22*, 2791. [Crossref]
37. Ji, M.; Liu, X.; Li, J.; Li, F.; Man, J.; Li, J.; Zhang, C.; Sun, K.; Qiu, Y.; *Mater. Lett.* **2023**, *348*, 134669. [Crossref]
38. Ogawa, K.; Yui, T.; Okuyama, K.; *Int. J. Biol. Macromol.* **2004**, *34*, 1. [Crossref]
39. Notin, L.; Viton, C.; David, L.; Alcouffe, P.; Rochas, C.; Domard, A.; *Acta Biomater.* **2006**, *2*, 387. [Crossref]
40. Hussain, S.; Kamran, M.; Khan, S. A.; Shaheen, K.; Shah, Z.; Suo, H.; Khan, Q.; Shah, A. B.; Rehman, W. U.; Al-Ghamdi, Y. O.; Ghani, U.; *Int. J. Biol. Macromol.* **2021**, *168*, 383. [Crossref]
41. Shechtman, O. In *Methods of Clinical Epidemiology*; Doi, S.; Williams, G., eds.; Springer: Berlin, Heidelberg, 2013. [Crossref]
42. Yan, A.; Xiao, X.; Külaots, I.; Sheldon, B. W.; Hurt, R. H.; *Carbon* **2006**, *44*, 3116. [Crossref]
43. Fajardo, A. R.; Lopes, L. C.; Rubira, A. F.; Muniz, E. C.; *Chem. Eng. J.* **2012**, *183*, 253. [Crossref]

Submitted: October 12, 2024
Published online: January 7, 2025